

The role of vicinal tyrosine residues in the function of *Haemophilus influenzae* ferric-binding protein A

Husain K. KHAMBATI*, Trevor F. MORAES†, Jagroop SINGH*, Stephen R. SHOULDICE‡, Rong-hua YU* and Anthony B. SCHRYVERS*¹

*Department of Microbiology and Infectious Diseases, University of Calgary, 3330 Hospital Drive NW, Calgary, Canada, T2N 4N1, †Department of Biochemistry, University of Toronto, 1 Kings College Circle, Toronto, Canada, M5S 1A8, and ‡Institute for Molecular Bioscience, The University of Queensland, 306 Camody Rd, Brisbane, QLD 4072, Australia

The periplasmic FbpA (ferric-binding protein A) from *Haemophilus influenzae* plays a critical role in acquiring iron from host transferrin, shuttling iron from the outer-membrane receptor complex to the inner-membrane transport complex responsible for transporting iron into the cytoplasm. In the present study, we report on the properties of a series of site-directed mutants of two adjacent tyrosine residues involved in iron co-ordination, and demonstrate that, in contrast with mutation of equivalent residues in the N-lobe of human transferrin, the mutant FbpAs retain significant iron-binding affinity regardless of the nature of the replacement amino acid. The Y195A and Y196A FbpAs are not only capable of binding iron, but are proficient in mediating periplasm-to-cytoplasm iron transport in a reconstituted FbpABC pathway in a specialized *Escherichia coli* reporter strain. This indicates that their inability to mediate iron acquisition from

transferrin is due to their inability to compete for iron with receptor-bound transferrin. Wild-type iron-loaded FbpA could be crystallized in a closed or open state depending upon the crystallization conditions. The synergistic phosphate anion was not present in the iron-loaded open form, suggesting that initial anchoring of iron was mediated by the adjacent tyrosine residues and that alternate pathways for iron and anion binding and release may be considered. Collectively, these results demonstrate that the presence of a twin-tyrosine motif common to many periplasmic iron-binding proteins is critical for initially capturing the ferric ion released by the outer-membrane receptor complex.

Key words: bacterial transferrin, ferric-binding protein A (FbpA), iron, periplasm, transferrin-binding protein (Tbp).

INTRODUCTION

Since iron is an essential element for many biological processes, there are a variety of specialized systems for transport, uptake and storage of this metal-ion cofactor in vertebrates that limit its availability to micro-organisms [1]. The primary mode of iron transfer throughout the body is via the glycoprotein transferrin. The transfer of iron to transferrin from dietary sources or from recycling pathways in the host is facilitated by ceruloplasmin or hephaestin, but transferrin is also capable of readily scavenging free ferric ion that it encounters. The ability to scavenge free ferric ion is also a characteristic feature of the related glycoprotein lactoferrin, particularly at sites of inflammation and other areas of lower pH [2]. Collectively, these proteins are responsible for sequestering free ferric ion in the host such that extracellular microbes require efficient iron-acquisition systems to survive and grow in the various ecological niches within the host.

Transferrin and lactoferrin are 80 kDa bi-lobed proteins, with each lobe being capable of binding a single iron atom. Each lobe is comprised of two structured domains that are connected by several β -strands with the site of iron binding at the base of the interdomain cleft. The β -strands facilitate substantial rigid-body conformational changes that range from a closed conformation with the domains in close juxtaposition to an open conformation involving rotational movements of up to 54° between the two domains [3]. The apoprotein is preferentially in the open conformation and, upon binding of a ferric ion to the C-terminal domain, a subsequent rotation of the N-terminal

domain completes the iron-co-ordination complex and stabilizes the iron-loaded form in the closed conformation [3].

The current model proposes that the process is initiated by binding of a synergistic carbonate anion to the C-terminal domain forming a cluster of four ligands that facilitate iron binding (two tyrosine residues and carbonate). The critical role of the synergistic anion is supported by biochemical studies with proteins altered in the anion-binding ligands [4]. Structural studies with iron-loaded camel lactoferrin in the open conformation, obtained by a microdialysis method, directly demonstrated that the bound iron atom is co-ordinated by two tyrosine residues and a carbonate anion [5]. Site-directed mutagenesis of the individual ligands involved in co-ordinating iron demonstrate that Tyr¹⁸⁸ of human transferrin is essential for binding, whereas mutation of Tyr⁹⁵ [6] or the histidine or glutamic acid residues [7,8] reduce, but do not eliminate, iron binding. The implication is that Tyr¹⁸⁸ is critical for the formation of the iron-co-ordination complex and may serve as the initial binding contact.

The release of iron from transferrin occurs in the endocytic vesicle, facilitated by the low pH. Protonation and release of the carbonate anion is proposed to be the first step in iron release, followed by protonation of the histidine ligand [9]. A pH-sensitive di-lysine trigger has also been proposed to be involved in the release of iron from transferrin [10], but previous studies suggest that the primary effect of mutation is to indirectly weaken iron co-ordination and facilitate the release of the synergistic anion [11]. In contrast with transferrin, lactoferrin retains iron at relatively low pH levels, consistent with its role in iron sequestration at sites of

Abbreviations used: ABC, ATP-binding cassette; FbpA, ferric-binding protein A; Tbp, transferrin-binding protein.

¹ To whom correspondence should be addressed (email schryver@ucalgary.ca)

The four refined crystal structures of FbpA determined in the present study will appear in the PDB under accession codes 3KN7 (Y195A), 3KN8 (Y196A), 3OD7 (wild-type closed) and 3ODB (wild-type open).

inflammation. The retention of iron at low pH has been attributed to co-operation between the two lobes in lactoferrin, which may be influenced in part by the α -helical connecting peptide between the lobes that is relatively non-structured in transferrin [3].

The periplasmic iron-binding proteins from *Haemophilus influenzae* and *Neisseria meningitidis* are considered 'bacterial transferrins' because of their structural similarity to a single lobe of transferrin or lactoferrin, consisting of two domains connected by a pair of antiparallel β -strands [12,13]. Analogous to transferrin, the ferric ion is co-ordinated by a similar set of ligands in an octahedral geometry: two tyrosine residues, a histidine residue, a glutamic acid residue, a phosphate anion and a water molecule. These Fbps (ferric-binding proteins) are essential for acquiring iron from host transferrin or lactoferrin [14,15] and are responsible for shuttling iron from an outer-membrane receptor complex, that binds to and removes iron from the host glycoprotein, to an inner-membrane transport complex that transports iron to the cytoplasm [16]. The outer-membrane complex, composed of a surface lipoprotein, TbpB (transferrin-binding protein B), and an integral outer-membrane protein, TbpA (transferrin-binding protein A), may simply release iron into the periplasm where it is efficiently scavenged by FbpA. However, recent studies demonstrating a TbpA–FbpA interaction [17] suggest that the iron from transferrin may be transferred directly from TbpA to FbpA. The inability of FbpA mutants with reduced iron-binding affinities to mediate acquisition of iron from transferrin [18] suggests that high-affinity binding by FbpA is required to drive the transport process and implies a competition between FbpA and receptor-bound transferrin. Although there is currently little information available on the inner-membrane transport complex or mechanism of iron removal from FbpA and transport across the inner membrane, it is likely that these involve the ATP-driven conformational changes and transport cycle proposed for ABC (ATP-binding cassette) importers [19]. However, it is not clear that domain separation alone would be sufficient for effective release of ferric ion bound to FbpA, thus a greater understanding of the iron-release process will be required.

In spite of different physiological roles, the similarities in structure and iron co-ordination between eukaryotic transferrins, lactoferrins and the bacterial transferrins [13] suggest that there may be common basic mechanisms for iron binding and release. Considerable insights into the mechanism of iron binding and release by transferrins and lactoferrins have been obtained through site-directed mutagenesis followed by structural and functional studies with the recombinant proteins [3]. This approach has been used less extensively to probe the iron-binding process of FbpA and to date has not yielded structures of the complete iron-co-ordination complex of mutant proteins in the closed conformation [18,20–22]. One apparent difference between human transferrin and FbpA is the role of the tyrosine ligands, as mutation of a single tyrosine residue eliminates iron-binding capabilities of the human transferrin N-lobe [6], but not of FbpA [18]. In the present study, a series of site-directed mutants of the conserved tyrosine ligands of FbpA were prepared to probe their role in iron binding under *in vitro* and *in vivo* conditions. In parallel, protein crystallography studies were pursued to obtain structures of iron-loaded proteins in the open and closed conformation to gain further insights into iron co-ordination.

EXPERIMENTAL

Further details are provided in the Experimental section in the Supplementary material at <http://www.BiochemJ.org/bj/432/bj4320057add.htm>. Mutant *H. influenzae fbpA* genes were

Table 1 Properties of wild-type and mutant FbpAs

The mass and molar absorption coefficients at 280 nm for the different FbpAs were calculated using the ProtParam tool on the ExPASy website (<http://www.expasy.ch/tools/protparam.html>). λ_{max} was identified from the absorption spectra and monitored in the citrate-competition experiments as described in the Supplementary Experimental section at <http://www.BiochemJ.org/bj/432/bj4320057add.htm>, yielding the indicated affinity constants. ND, not detectable.

FbpA	Mass absorption coefficient	Molar absorption coefficient	λ_{max} (nm)	Affinity constant (log K_a)
Wild-type	33685.2	41370	480	19.62 \pm 0.07
Y195A	33593.1	39880	466	19.41 \pm 0.12
Y195H	33659.1	39880	472	19.36 \pm 0.08
Y195I	33635.2	39880	461	19.27 \pm 0.01
Y195F	33669.2	39880	478	19.22 \pm 0.03
Y195E	33651.1	39880	480	18.87 \pm 0.09
Y196A	33593.1	39880	471	19.20 \pm 0.04
Y196H	33659.1	39880	463	19.05 \pm 0.04
Y196I	33635.2	39880	461	18.97 \pm 0.17
Y196F	33669.2	39880	457	18.96 \pm 0.08
Y196E	33651.1	39880	465	18.92 \pm 0.14
Y195A, Y196A	33501.0	38390	None	ND

prepared by SOEing (splicing by overlap extension) PCR or the QuikChange™ mutagenesis protocol and subcloned into a vector used for protein production. The recombinant FbpA proteins were expressed at high levels in the *Escherichia coli* periplasm, and pure preparations of protein were obtained after ion-exchange chromatography for spectral analyses and crystallography. Spectra were obtained for iron-loaded preparations of FbpAs, and the iron-binding properties were assessed using a citrate-competition assay (Table 1). As described more fully in the Supplementary Experimental section, Supplementary Table S1 at <http://www.BiochemJ.org/bj/432/bj4320057add.htm>, and the Results section below, the purified FbpA preparations were also used in crystallization screens and structures of several wild-type and mutant FbpAs were determined. The four refined crystal structures of FbpA determined for the present study have been deposited in the PDB under the accession codes 3KN7 (Y195A), 3KN8 (Y196A), 3OD7 (wild-type closed) and 3ODB (wild-type open). For statistics, see Supplementary Table S2 at <http://www.BiochemJ.org/bj/432/bj4320057add.htm>.

In order to evaluate the function of mutant FbpAs in iron acquisition, QuikChange™ mutagenesis was performed directly on a plasmid encoding the entire FbpABC pathway [23] and the resulting plasmids were used to transform a specialized reporter strain defective in iron transport [24].

RESULTS

Properties of the site-directed mutant FbpAs

The two tyrosine ligands (Tyr¹⁹⁵ and Tyr¹⁹⁶) of the 'bacterial transferrin', FbpA from *H. influenzae*, were targeted for site-directed mutagenesis in order to evaluate their contribution to iron co-ordination and compare it with that of vertebrate transferrins and lactoferrins. A set of site-directed mutants of Tyr¹⁹⁵ and Tyr¹⁹⁶ were designed to provide a range of amino acid replacements of varying size and properties (Table 1). The combination of high-level expression by the T7 expression system and efficient export into the periplasmic space provides a facile method for obtaining relatively pure preparations of FbpA. The level of production is usually in the 50–150 mg/l range and wild-type FbpA usually constitutes > 80% of the protein in the osmotic-shock fluid as assessed by SDS/PAGE (results not shown). Although there was

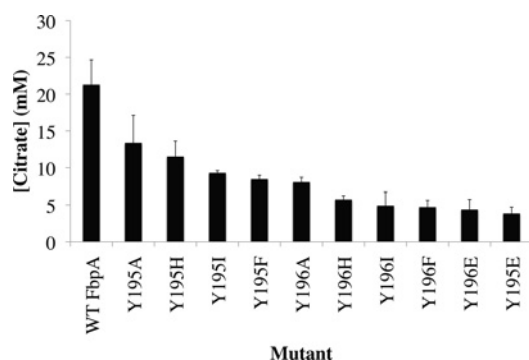


Figure 1 Citrate-competition assay

The concentration of citrate required to remove 50% of the iron from FbpA was determined as described in the Supplementary Experimental section at <http://www.BiochemJ.org/bj/432/bj4320057add.htm>. Results shown are means \pm S.D. from three independent experiments.

a 2–3-fold variation in the level of protein expression for the different FbpAs, this may not reflect differences in protein stability, but, instead, the inherent variation in expression with this system. The purity of the proteins after ion exchange was comparable and, as there was no indication of instability of the resulting preparations, it was unlikely to have an impact on the results.

As a first step for probing the iron-binding properties of the different FbpA proteins, the purified protein preparations were subjected to the iron-loading procedure and the UV-visible (300–800 nm) spectra were determined. After removing the excess iron, colour was observed in all the protein samples except the Y195A/Y196A double mutant and a peak in the spectra in the 450–480 nm range was evident for the other mutants (Table 1). The λ_{max} is inversely proportional to the energy of the charge-transfer band for the iron–tyrosine residue interaction. The absorption bands for all the mutants with the exception of Y195E have a considerable blue shift; such a shift suggests an increased Tyr(O)–Fe interaction with the remaining tyrosine residue. Since the Y195A/Y196A double mutant does not contain any iron-coordinating tyrosine residues, there are no detectable spectral changes, which is a useful control for the spectral measurements, but does not provide any information regarding iron binding.

In order to obtain an overall estimation of the iron-binding affinity of the mutant proteins, citrate-competition assays were performed. In this assay, 100 μM iron-loaded protein was exposed to varying concentrations of citrate (0.5–500 mM). This assay provides a relative measure of iron-binding affinity of the various mutants and the strength of the tyrosine residue–iron interaction. The concentration required to remove 50% of the iron for the mutant proteins is illustrated in Figure 1. The titration with citrate can be used to estimate the iron-binding constants for the mutant proteins, which ranged from 18.92 to 19.62 (Table 1) [25]. It is salient to note that the present assay was performed at pH 8 to facilitate comparison with previous studies, but that the pH of the periplasm would normally be substantially lower and have an impact on the binding constants.

Mutations that replaced tyrosine residues with histidine or glutamic acid were included to provide the potential to co-ordinate iron, whereas isoleucine, phenylalanine and alanine residues would eliminate one iron-coordinating ligand. The potential for iron co-ordination clearly did not result in enhanced retention of iron as the mutant proteins with glutamic acid had the weakest iron-binding properties (Figure 1 and Table 1), and for each tyrosine residue, the alanine replacement tended to have the strongest binding. The overall trend for both Tyr¹⁹⁵ and Tyr¹⁹⁶ was

Ala>His>Ile>Phe>Glu. The results suggest that the different side-chain replacements may be perturbing the iron-co-ordination geometry to varying degrees, indicating that structural studies will be required to explore the details of iron co-ordination in the various mutants.

It is clear that, irrespective of which amino acid is used to replace tyrosine, mutation of either of the neighbouring tyrosine residues does not abrogate iron binding (Figure 1 and Table 1), in contrast with what has been demonstrated for the N-lobe of human transferrin [6].

Pathway-reconstitution studies

Although the tyrosine mutants retain substantial iron-binding capabilities based on the *in vitro* binding studies (Figure 1 and Table 1), previous studies indicate that they are defective in supporting growth on transferrin or ferric citrate medium [18]. The growth properties of *H. influenzae* expressing the Y195A or Y196A mutant proteins on iron-limited anaerobic growth medium were not distinguishable from a strain lacking an FbpA protein. This implies that there is either a deficiency in acquiring iron in the periplasm or a deficiency in donating iron to the inner-membrane complex composed of FbpB and FbpC. However, the inability to detect a difference between growth of strains expressing the mutant FbpAs and strains lacking FbpA does not necessarily imply that they are totally defective in iron transport. The presence of alternate iron pathways could readily obscure any enhancement that transport with the tyrosine mutant FbpAs would provide over an FbpABC pathway lacking FbpA. Thus an alternate-pathway-reconstitution approach was sought to address this issue.

An *E. coli* reporter strain, H1771, that is defective in iron uptake [24] has been used successfully to identify foreign ferric and ferrous ion-uptake pathways [26] and was selected for pathway-reconstitution experiments. This reporter strain is defective in a ferrous ion-uptake pathway (Feo-negative), resulting in reduced levels of intracellular iron, which is monitored by the presence of a β -galactosidase reporter gene fused to the Fur-regulated promoter region of the *fhuF* gene. There are substantial levels of β -galactosidase activity even when this strain is grown in medium containing high levels of exogenous iron, and thus repression of expression is dependent on the introduction of a functional iron-transport pathway. Preliminary experiments with plasmid pSC590 encoding the *H. influenzae* *fbpABC* operon [23] demonstrated the utility of this approach, as colonies of transformants with this plasmid were white on specialized MacConkey plates, compared with the red colony colour of the parent reporter strain. The presence of this vector resulted in substantial repression of β -galactosidase expression in cells grown on iron-supplemented medium (914–1345 units compared with cells carrying the control plasmid with 230915–254302 units). Thus it was decided to test the ability of this system to compare the function of mutant FbpAs (Figure 2).

The *fbpA* gene in the pSC590 vector was mutated using QuikChange™ mutagenesis as described in the Supplementary Experimental section. In order to account for any iron transport mediated by the FbpBC inner-membrane complex, a control plasmid was introduced in which two stop codons had been inserted in place of the tyrosine residues in the gene encoding FbpA (YYSTOP).

To evaluate the effect of mutation of the tyrosine residues, the pSC590 plasmid was mutagenized and transformed into strain H1771, producing the following derivatives: the Y195A mutant, the Y196A mutant and the Y195A/Y196A double mutant (YYAA). Three or more colonies were selected from several transformations for analysis in order to account for variability

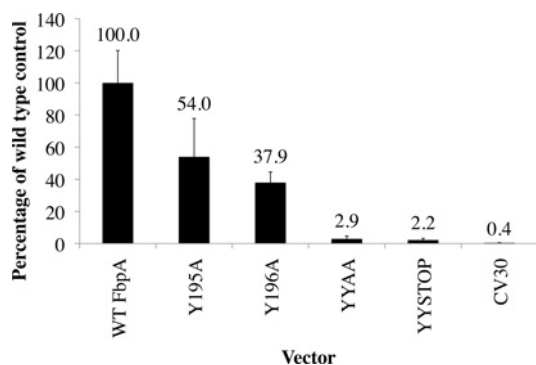


Figure 2 Inhibition of β -galactosidase activities of strains expressing mutant FbpAs

The reporter strain was transformed with control plasmid (CV30), plasmid encoding the native FbpA (WT), mutant FbpA (Y195A or Y196A), double-mutant Y195A/Y196A FbpA (YYAA) or FbpA with two stop codons (YYSTOP). β -Galactosidase activities were calculated in Miller units, used to calculate the inverse and expressed as a percentage of the control values. Results are means \pm S.D. from three independent experiments.

in the assay. The results illustrated in Figure 2 demonstrate that both of the Y195A and Y196A proteins are capable of acquiring iron in the *E. coli* periplasm and donating the iron to the inner-membrane transport complex. In contrast, the level of β -galactosidase activity in the strain expressing the double-mutant protein (YYAA) is comparable with the strain carrying the mutant gene containing stop codons (YYSTOP). This indicates that the Y195A/Y196A mutant FbpA is defective in iron binding or in donation to the inner-membrane transport complex, logically the former. The small residual amount of β -galactosidase activity in these cells relative to the empty vector (CV30) may be due to the presence of the functional FbpBC complex.

Although this assay was effective at addressing the questions posed, the results in Figure 2 illustrate that it may be limited in making comparisons between the different mutations. Owing to the experimental variation in the current assay, it is not possible to conclude that the Y195A FbpA is more effective at mediating iron acquisition than the Y196A FbpA. Thus it was not deemed appropriate for comparing the function of the various mutant FbpAs described in the previous section. It is evident that an alternate reporter system will need to be developed in order to be able to effectively compare these various mutant FbpAs.

Structural studies

Structural studies with site-directed mutants of human lactoferrin and human transferrin have provided considerable insights into iron co-ordination, as the mutant proteins crystallized in the closed conformation [7,8]. In contrast, structural studies with site-directed mutants of *H. influenzae* FbpA yielded structures of the mutant proteins in the open conformation [20–22], so information on how the mutation influenced the formation of the iron co-ordination complex is lacking. Therefore a strategy was pursued to use crystals of the wild-type protein in the closed conformation to seed formation of crystals of the mutant proteins. Crystallization setups using a common preparation of wild-type iron-loaded FbpA were prepared with an imidazole/malate buffer that was used in the first published study [12] and with a methyl ethane sulfonate buffer used in structural studies of the mutant proteins [22]. Coloured crystals of the wild-type protein were readily obtained and used in a variety of different seeding strategies with the mutant proteins. The wild-type crystals and mutant crystals were subjected to X-ray diffraction analysis and

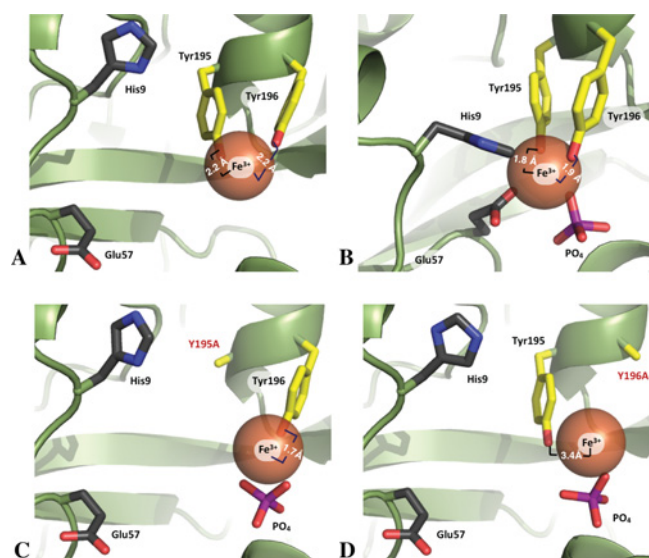


Figure 3 Iron-co-ordination complex of FbpAs, showing Tyr¹⁹⁵-OH-Fe and Tyr¹⁹⁶-OH-Fe bond distances

(A) Holo-FbpA crystallized in the open conformation (PDB code 30DB). (B) Holo-FbpA crystallized in the closed conformation (PDB code 30D7). (C) Y195A mutant FbpA (PDB code 3KN7). (D) Y196A mutant FbpA (PDB code 3KN8). 1 Å = 0.1 nm.

unit cell dimensions were determined as these could be used to discriminate between the closed and open conformations of FbpA (see the Supplementary Experimental section). Surprisingly, the only crystals in the closed conformation based on this analysis was the wild-type protein crystallized with the imidazole/malate buffer, suggesting that the wild-type protein crystallized in the methyl ethane sulfonate buffer was in the open conformation, yet contained bound iron.

Crystals of the wild-type protein in the closed conformation were prepared and used to seed the formation of crystals of mutant proteins, including the Q58L FbpA as this mutation had the least impact on iron binding [18]. Although crystals were obtained in a variety of conditions with different mutant proteins, the crystals obtained under the seeding conditions had unit cell dimensions, indicating that the proteins were in the open conformation. The failure to obtain crystals of the mutant proteins in the closed conformation after repeated attempts at seeding suggested that it would be unlikely to obtain crystals of mutant proteins in the closed conformation, even after extensive screening, and prompted us to abandon these efforts.

The initial X-ray diffraction results suggesting that the wild-type iron-loaded FbpA crystallized in the open conformation were surprising since the iron-loaded forms of native transferrins, lactoferrins and periplasmic iron-binding proteins have crystallized in the closed conformation, except when specialized approaches were taken [5,27]. The same preparation of wild-type FbpA was used for the generation of crystals in the closed and open forms, indicating that crystallization in the open conformation was not due to modifications during the production and purification processes. Since comparison of the structures of the open and closed forms of the protein might provide insights into the molecular events involved in iron binding, additional datasets were collected and the structures were determined by molecular replacement using Molrep.

The structure of wild-type FbpA in the open conformation revealed that the iron atom was co-ordinated by the adjacent tyrosine residues in the C-domain and that there was no phosphate anion present in the anion-binding pocket (Figure 3A). The

structure of FbpA in the closed conformation from the same preparation (Figure 3B) had a complete iron co-ordination complex, including the synergistic phosphate anion. These results indicate that the synergistic phosphate anion is not required for binding of ferric ion by the tyrosine residues in the C-terminal domain, and may imply that initial anchoring of the ferric ion is mediated by the tyrosine residues. The phosphate anion clearly stabilizes the co-ordination of the ferric ion and, through interactions with residues in the N-terminal domain, maintenance of the closed conformation. One possible explanation for the presence of phosphate when FbpA crystallized in the closed conformation and its absence when FbpA was present in the open conformation is that there may have been limited phosphate available in the crystallization mixtures and phosphate would strongly favour binding to protein in the closed conformation. Thus any phosphate associated with FbpA in the open conformation that was added to the crystal lattice would tend to equilibrate with free FbpA capable of assuming the closed conformation.

Although it was not possible to obtain crystals of mutant proteins in the closed conformation, we decided to determine the structure of the Y195A and Y196A mutant FbpAs to gain insights into the anchoring of the ferric ion by the remaining tyrosine residue. As described in the Supplementary Experimental section, crystals with good diffraction properties were obtained using preparations and conditions similar to those used previously for other FbpA mutants [21,22]. The structures of the iron co-ordination site of the Y195A and Y196A FbpA are illustrated in Figures 3(C) and 3(D) respectively. In both of these structures, the ferric ion is co-ordinated by the remaining tyrosine residue and the synergistic phosphate anion. The presence of this anion may have been biased by the inclusion of exogenous phosphate in the protein preparation used for these crystals [21]. It is salient to note that the OH-Fe bond between Tyr¹⁹⁶ and the ferric ion in the Y195A mutant protein is considerably shorter than the OH-Fe bond between Tyr¹⁹⁵ and the ferric ion in the Y196A mutant protein. This may explain the higher affinity for iron binding by the Y195A protein (Table 1 and Figure 1).

DISCUSSION

Eukaryotic transferrins and the 'bacterial transferrins', FbpAs from *H. influenzae* and the pathogenic *Neisseria* species, have similar means of achieving high-affinity binding of ferric ions, which is essential for their respective physiological roles. The iron-binding site is composed of a similar set of ligands positioned at the base of a cleft between two rigid domains that fluctuate between open and closed conformations, with the iron-loaded form predominantly in the closed conformation and the apo form predominantly in the open conformation [28,29]. The ligands involved in co-ordinating iron are from both the N-terminal and C-terminal domains and thus contribute to maintaining the iron-loaded form in the closed conformation. Structures have been obtained of iron-free lobes of lactoferrin in various states of closure [3], and mutants of transferrin defective in the iron co-ordinating ligands crystallized in the closed conformation [7,8], suggesting that other interactions contribute to stabilizing the closed conformation. In contrast, structures of mutants in the iron-co-ordinating ligands of FbpA have uniformly been in the open conformation [18,20–22,30] and, despite our best efforts, we were unable to capture mutant proteins in the closed conformation even when seeding with microcrystals in the closed conformation. The shallower cleft and less-extensive domain interface of FbpAs may make the domain closure more

dependent upon the ligands co-ordinating the iron and synergistic anion than for transferrins and lactoferrins and may need to be considered when making mechanistic comparisons.

H. influenzae and the pathogenic *Neisseria* species are capable of using human transferrin as a sole source of iron for growth by an iron-acquisition process mediated by a human transferrin-specific surface receptor [31]. The receptor is composed of a TonB-dependent integral membrane protein, TbpA, and a lipid-anchored surface lipoprotein, TbpB. The receptor binds transferrin, removes iron and transports it across the outer membrane where it is bound by FbpA for subsequent donation of iron to the inner-membrane transport complex. The proposal that binding to the receptor would induce conformational changes (domain separation) in transferrin that lowers the affinity for binding iron [32] is supported by studies with isolated receptor proteins [33] or membranes containing receptor proteins [17] in which transfer of iron to FbpA only occurs in the presence of the receptor proteins. The recent demonstration that apo FbpA preferentially binds to membranes containing TbpA [17] and that the transport process requires a threshold of iron-binding affinity [18] suggests that there may be competition for iron between transferrin and FbpA bound to the TbpA protein. Thus delineation of the mechanism of iron removal and transport by the receptor will rely on detailed comparisons between the iron-binding mechanisms of transferrin and FbpA.

Previous studies have demonstrated that Tyr¹⁸⁸ in the human transferrin N-lobe is essential for iron binding [6], suggesting that it may be the residue responsible for initial anchoring of the ferric ion or that there is insufficient flexibility in the iron-binding pocket on the C-terminal domain to accommodate other ligands. In contrast, mutation of either of the adjacent tyrosine residues with a variety of different replacement amino acids does not abrogate iron binding by FbpA (Table 1 and Figure 1). It is interesting to note that the mutants with an alanine residue replacing tyrosine retained the highest affinity for binding iron, suggesting that providing some 'flexibility' in the iron co-ordination sphere may be advantageous. Structural studies demonstrate that the ferric ion is bound by the remaining tyrosine residue and synergistic anion in the C-terminal domain (Figures 3C and 3D), indicating that either tyrosine residue can serve as the initial anchoring ligand. These two adjacent tyrosine residues are present in structures from periplasmic iron-binding proteins from a variety of species, including *Serratia marcescens*, *Yersinia enterocolitica* [34], *Mannheimia haemolytica* [35] and *Campylobacter jejuni* [36], that include a diversity of different modes of iron co-ordination. This indicates that the adjacent tyrosine residues provide a versatile means of anchoring an iron atom with flexibility in accommodating modifications to the iron-co-ordination scheme. Bioinformatics analyses indicate that the 'twin tyrosine' motif is widespread among homologues in a diversity of different species and, at present, other modes of iron co-ordination in periplasmic iron-binding proteins have not been identified.

In the present study, we not only show that the Y195A and Y196A mutant FbpAs are capable of binding iron (Table 1 and Figure 1), but also demonstrate that these proteins are capable of mediating transport of iron from the periplasm to cytoplasm in a reconstituted pathway (Figure 2). Thus their apparent inability to mediate iron acquisition from transferrin in a reconstituted pathway in *H. influenzae* [18] is probably due to an inability to compete with receptor-bound transferrin for iron as was observed with the H9A and E57A mutants. In the previous study [18], strains expressing the Y195A and Y196A proteins grew at the same level of exogenous ferric citrate as the strain lacking an FbpA protein, inferring that they were not capable of mediating

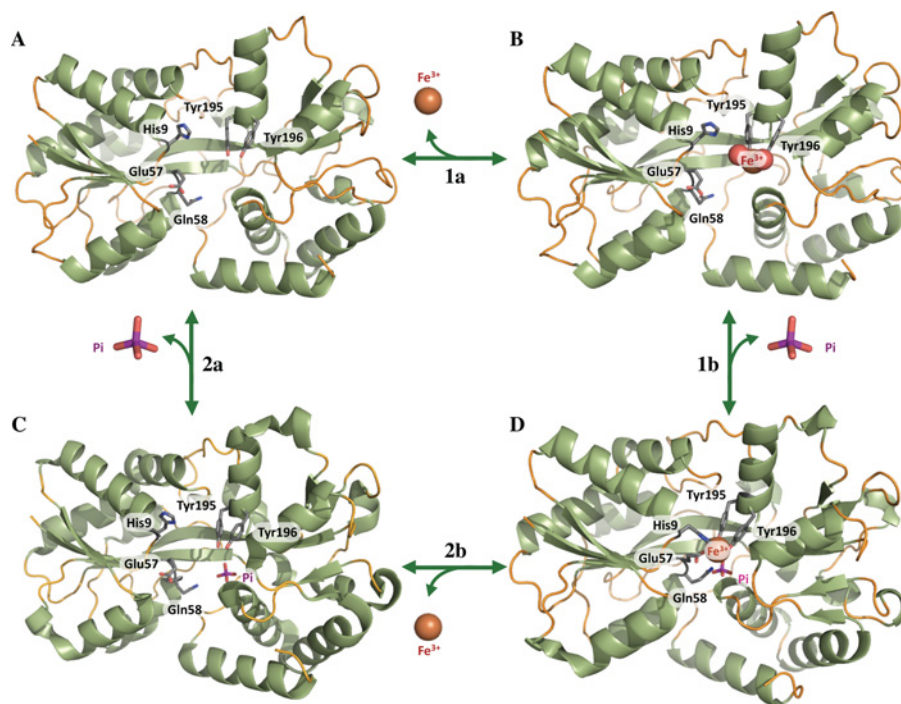


Figure 4 Models for iron binding by *H. influenzae* FbpA under low- and high-phosphate conditions

Under phosphate-limited conditions, FbpA is in an iron-free phosphate-free open conformation (A). Iron released into the periplasm (1a) binds iron through the tyrosine ligands on the C-terminal domain (B). Preferential binding of available phosphate by the Fe–FbpA complex (1b) results in closure of the domains and completion of the iron-co-ordination complex (D). In the presence of high concentrations of phosphate (2a), FbpA contains bound phosphate (C), facilitating iron co-ordination and domain closure upon iron binding (2b), resulting in a holo form of FbpA proficient in binding to the inner-membrane transport complex.

iron transport. However, in light of the results from the present study, it seems more likely that there are alternate iron-uptake pathways in wild-type *H. influenzae* that are equally capable of acquiring iron as the FbpABC pathway when the Y195A and Y196A FbpA mutant proteins are present. It is salient to remember that the *E. coli* reporter strain is defective in iron uptake, which enabled us to detect iron uptake mediated by the FbpABC pathway. This highlights clear advantages that the reporter strain has in monitoring iron acquisition and that there may be value in developing a variety of different reporter strains in different bacterial species.

There is considerable evidence that the synergistic carbonate anion plays a significant role in the initial capture of ferric ion by the C-terminal domain of transferrin and lactoferrin lobes [4,5]. Similarly, the presence of a phosphate anion in the published structures of the apo and iron-loaded forms of the *H. influenzae* FbpA [12,29] combined with experimental evidence for a strong preference for the phosphate anion [37] argue for a critical role of the phosphate anion in iron binding. However, the absence of phosphate in the iron-loaded wild-type FbpA in the open conformation (Figure 3) indicates that the presence of phosphate in structural studies may be a function of the conditions of protein preparation and crystallization. In structures containing a synergistic phosphate anion, exogenous phosphate was either added to the samples prior to crystal setups or in buffers used in the purification protocol. In contrast with the kinetic studies that argue for the important role of the synergistic anion, site-directed mutants defective in phosphate binding were fully capable of growth on transferrin iron [20]. Furthermore, although the preparation and crystallization conditions were similar, phosphate was absent from structures of the N175L and N193L mutant proteins while present in the structure of the Q58L

mutant, as this residue is on the N-terminal domain. These results, combined with the phosphate-negative open structure obtained in the present study, collectively indicate that, although phosphate may commonly participate in the iron-transport process, it is neither integral nor essential for iron binding or iron acquisition. Considering that these bacteria will be in relatively phosphate-rich environments during invasion or when occupying the submucosal environment of the respiratory tract, but may encounter more-variable conditions when colonizing the mucosal surface, having the flexibility to function without phosphate but operate more efficiently in its presence would be a useful feature for FbpA.

A recent study probing the binding of ferric anion complexes by wild-type and mutant FbpAs from *Neisseria gonorrhoeae* with time-resolved stopped-flow absorbance and fluorescence spectroscopy demonstrated that the phosphate anion altered the stages and kinetics of binding and led the authors to conclude that initial binding involved ligands in the N-terminal domain [38]. In contrast, our results with the wild-type protein crystallizing in the open conformation (Figure 3A) as well as previous structural studies with mutant FbpAs [20,21,22] strongly argue for the initial binding to the tyrosine residues in the C-terminal domain, as the structures clearly show iron bound to the tyrosine residues with the N-terminal ligands pointing away from the binding site. Our interpretation is that this represents an intermediate stage in iron binding, which requires domain closure to complete the optimal iron-co-ordination complex. We believe that there are alternate interpretations of the kinetic data from the previous study that are consistent with binding to residues in the C-lobe.

In the present study, we obtained structures of iron-loaded wild-type FbpA in the open (Figure 4B) and the closed (Figure 4D) conformations from the same preparation, which could potentially represent different stages in the iron-binding and-release process.

The published structure of the apo form of FbpA [29] (Figure 4B) and a structure lacking the bound phosphate (Figure 4A) represent additional stages of proposed pathways for iron binding under limiting phosphate (1a and 1b, Figure 4) or sufficient phosphate (2a and 2b, Figure 4) conditions.

Under phosphate-limited conditions that potentially could exist on the mucosal surface, the apo form of FbpA in the periplasm would not contain the phosphate anion (Figure 4A) and ferric ion released from transferrin by the outer-membrane transport complex would bind directly to the tyrosine ligands in the C-terminal domain (1a, Figure 4B). The transfer of ferric ion from TbpA to FbpA would probably involve a 'solubilizing' anion, which might be determined by relative concentrations in the periplasm. Available phosphate would be preferentially bound by the resulting ferric ion–FbpA complex, facilitating completion of the octahedral binding pocket by closure of the two lobes through successive co-ordination of iron by the glutamic acid and histidine ligands and engagement of the glutamic acid in phosphate co-ordination (1b, Figure 4D). The crystallization conditions lacking added phosphate that we used for our structural studies resulted in bound phosphate being present in FbpA in the closed conformation (Figure 4D), supporting the proposal for efficient capture of available phosphate by the Fe–FbpA complex.

Bacteria in the submucosal space or in other body compartments during invasive disease would be exposed to relatively high levels of phosphate such that periplasmic FbpA would contain a bound phosphate anion (2a, Figure 4C). The bound phosphate anion would facilitate binding of ferric ion (2b, Figure 4) and rapid formation of the octahedral iron-co-ordination complex through domain closure (Figure 4D). The process of iron removal by the inner-membrane transport complex is unknown, but the important role that the phosphate anion plays in iron co-ordination might be exploited by displacement of the bound phosphate anion to facilitate the removal of the bound iron atom (Figure 4, reversal of 1b and 1a).

As illustrated in the present study, the relative ease of production of site-directed mutants of FbpAs for biochemical and structural studies, and the ability to test their function in a reconstituted iron-uptake pathway, provides a powerful approach for probing the mechanisms of iron binding and release. However, the inability to crystallize iron-bound mutant proteins in the closed conformation limits the ability to delineate the detailed impact of specific mutations on iron co-ordination. Our results also indicate that one has to be careful about predicting the impact of specific mutations on iron-binding properties and suggest that there may be flexibility in achieving iron binding. We propose that the consistent association of iron with tyrosine residues in the C-terminal domain in structures of wild-type and mutant FbpAs, and the conserved di-tyrosine motif in other periplasmic iron-binding proteins, strongly argues for the critical role of the tyrosine residues in initial anchoring of the ferric ion. More-direct experimental evidence than kinetic analyses [38] will be needed to support the proposal that iron is initially bound by residues in the N-terminal domain.

AUTHOR CONTRIBUTION

Anthony Schryvers was responsible for the development of the research programme, and provided supervision and guidance in implementation of the research and assistance in initial crystallization screens. Trevor Moraes provided direction and assistance in the crystallization experiments and collection of the diffraction data, and was largely responsible for solving the structures of apo and holo wild-type FbpAs. Stephen Shouldice independently solved the structures of the mutant FbpAs. Rong-hua Yu generated most of the site-directed mutations and prepared the wild-type and mutant proteins for crystallization screens. Husain Khambati, with some assistance from Jagroop

Singh, subcloned the mutant genes and produced the proteins for spectral analyses, and also prepared mutant genes and performed the pathway-reconstitution experiments; with assistance from Trevor Moraes and Anthony Schryvers, he performed the structural studies with the wild-type FbpA and the attempts at crystallizing mutant proteins in the closed conformation.

ACKNOWLEDGEMENTS

We thank Dr Natalie Strynadka (Department of Biochemistry and Molecular Biology, University of British Columbia, Vancouver, BC, Canada) for the use of the X-ray diffractometer, and Hyo Jong Park for her assistance in the purification of the FbpA mutants.

FUNDING

This work was supported by the Canadian Institutes of Health Research [grant number 49603].

REFERENCES

- Schaible, U. E. and Kaufmann, S. H. (2004) Iron and microbial infection. *Nat. Rev. Microbiol.* **2**, 946–953
- Ward, P. P. and Conneely, O. M. (2004) Lactoferrin: role in iron homeostasis and host defense against microbial infection. *Biomaterials* **17**, 203–208
- Baker, H. M. and Baker, E. N. (2004) Lactoferrin and iron: structural and dynamic aspects of binding and release. *Biomaterials* **17**, 209–216
- Zak, O., Ikuta, K. and Aisen, P. (2002) The synergistic anion-binding sites of human transferrin: chemical and physiological effects of site-directed mutagenesis. *Biochemistry* **41**, 7416–7423
- Khan, J., Kumar, P., Srinivasan, A. and Singh, T. (2001) Protein intermediate trapped by the simultaneous crystallization process. *J. Biol. Chem.* **276**, 36817–36823
- He, Q. Y., Mason, A. B., Woodworth, R. C., Tam, B. M., MacGillivray, R. T. A., Grady, J. K. and Chasteen, N. D. (1997) Inequivalence of the two tyrosine ligands in the N-lobe of human serum transferrin. *Biochemistry* **36**, 14853–14860
- Nicholson, H., Anderson, B. F., Bland, T., Shewry, S. C., Tweedie, J. W. and Baker, E. N. (1997) Mutagenesis of the histidine ligand in human lactoferrin: iron binding properties and crystal structure of the histidine-253→methionine mutant. *Biochemistry* **36**, 341–346
- Faber, H. R., Bland, T., Day, C. L., Norris, G. E., Tweedie, J. W. and Baker, E. N. (1996) Altered domain closure and iron binding in transferrins: the crystal structure of the Asp60Ser mutant of the amino-terminal half-molecule of human lactoferrin. *J. Mol. Biol.* **256**, 352–363
- Jeffrey, P. D., Bewley, M. C., MacGillivray, R. T. A., Mason, A. B., Woodworth, R. C. and Baker, E. N. (1998) Ligand-induced conformational change in transferrins: crystal structure of the open form of the N-terminal half-molecule of human transferrin. *Biochemistry* **37**, 13978–13986
- He, Q. Y., Mason, A. B., Tam, B. M., MacGillivray, R. T. A. and Woodworth, R. C. (1999) Dual role of Lys²⁰⁶–Lys²⁹⁶ interaction in human transferrin N-lobe: iron-release trigger and anion-binding site. *Biochemistry* **38**, 9704–9711
- Baker, H. M., Nurizzo, D., Mason, A. B. and Baker, E. N. (2007) Structures of two mutants that probe the role in iron release of the dilysine pair in the N-lobe of human transferrin. *Acta Crystallogr. D Biol. Crystallogr.* **63**, 408–414
- Bruns, C. M., Norwalk, A. J., Avrai, A. S., McTigue, M. A., Vaughan, K. A., Mietzner, T. A. and McRee, D. E. (1997) Structure of *Haemophilus influenzae* Fe⁺³-binding protein reveals convergent evolution within a superfamily. *Nat. Struct. Biol.* **4**, 919–924
- Taboy, C. H., Vaughan, K. G., Mietzner, T. A., Aisen, P. and Crumbliss, A. L. (2001) Fe³⁺ coordination and redox properties of a bacterial transferrin. *J. Biol. Chem.* **276**, 2719–2724
- Khun, H. H., Kirby, S. D. and Lee, B. C. (1998) A *Neisseria meningitidis* fbpABC mutant is incapable of using nonheme iron for growth. *Infect. Immun.* **66**, 2330–2336
- Kirby, S. D., Gray-Owen, S. D. and Schryvers, A. B. (1997) Characterization of a ferric binding protein mutant in *Haemophilus influenzae*. *Mol. Microbiol.* **25**, 979–987
- Lau, G. H., MacGillivray, R. T. and Murphy, M. E. (2004) Characterization of a nucleotide-binding domain associated with neisserial iron transport. *J. Bacteriol.* **186**, 3266–3269
- Silburt, C., Roulhac, P., Weaver, K., Noto, J., Mietzner, T., Cornelissen, C., Fitzgerald, M. and Crumbliss, A. (2009) Hijacking transferrin bound iron: protein-receptor interactions involved in iron transport in *N. gonorrhoeae*. *Metallomics* **1**, 249–255
- Khan, A. G., Shouldice, S. R., Kirby, S. M., Yu, R. -H., Tari, L. W. and Schryvers, A. B. (2007) High-affinity binding by the periplasmic iron-binding protein from *Haemophilus influenzae* is required for acquiring iron from transferrin. *Biochem. J.* **404**, 217–225

- 19 Rees, D. C., Johnson, E. and Lewinson, O. (2009) ABC transporters: the power to change. *Nat. Rev. Mol. Cell Biol.* **10**, 218–227
- 20 Khan, A. G., Shouldice, S. R., Tari, L. W. and Schryvers, A. B. (2007) The role of the synergistic phosphate anion in iron transport by the periplasmic iron-binding protein from *Haemophilus influenzae*. *Biochem. J.* **403**, 43–48
- 21 Shouldice, S. R., Dougan, D. R., Skene, R. J., Tari, L. W., McRee, D. E., Yu, R. -H. and Schryvers, A. B. (2003) High resolution structure of an alternate form of the ferric-ion binding protein from *Haemophilus influenzae*. *J. Biol. Chem.* **278**, 11513–11519
- 22 Shouldice, S. R., Skene, R. J., Dougan, D. A., McRee, D. E., Tari, L. W. and Schryvers, A. B. (2003) The presence of ferric-hydroxide clusters in mutants of the *Haemophilus influenzae* ferric ion-binding protein A. *Biochemistry* **42**, 11908–11914
- 23 Adhikari, P., Kirby, S. D., Nowalk, A. J., Veraldi, K. L., Schryvers, A. B. and Mietzner, T. A. (1995) Biochemical characterization of a *Haemophilus influenzae* periplasmic iron transport operon. *J. Biol. Chem.* **42**, 25142–25149
- 24 Hantke, K. (1987) Selection procedure for deregulated iron transport mutants (*fur*) in *Escherichia coli* K 12: *fur* not only affects iron metabolism. *Mol. Gen. Genet.* **210**, 135–139
- 25 Chen, C. -Y., Berish, S. A., Morse, S. A. and Mietzner, T. A. (1993) The ferric iron-binding protein of pathogenic *Neisseria* spp. functions as a periplasmic transport protein in iron acquisition from human transferrin. *Mol. Microbiol.* **10**, 311–318
- 26 Wyckoff, E. E., Mey, A. R., Leimbach, A., Fisher, C. F. and Payne, S. M. (2006) Characterization of ferric and ferrous iron transport systems in *Vibrio cholerae*. *J. Bacteriol.* **188**, 6515–6523
- 27 Zhu, H., Alexeev, D., Hunter, D. J., Campopiano, D. J. and Sadler, P. J. (2003) Oxo-iron clusters in a bacterial iron-trafficking protein: new roles for a conserved motif. *Biochem. J.* **376**, 35–41
- 28 MacGillivray, R. T. A., Moore, S. A., Chen, J., Anderson, B. F., Baker, H., Luo, Y. G., Bewley, M., Smith, C. A., Murphy, M. E. P., Wang, Y. et al. (1998) Two high-resolution crystal structures of the recombinant N-lobe of human transferrin reveal a structural change implicated in iron release. *Biochemistry* **37**, 7919–7928
- 29 Bruns, C. M., Anderson, D. S., Vaughan, K. G., Williams, P. A., Nowalk, A. J., McRee, D. E. and Mietzner, T. A. (2001) Crystallographic and biochemical analyses of the metal-free *Haemophilus influenzae* Fe³⁺-binding protein. *Biochemistry* **40**, 15631–15637
- 30 Ekins, A., Khan, A. G., Shouldice, S. R. and Schryvers, A. B. (2004) Lactoferrin receptors in Gram-negative bacteria: insights into the iron acquisition process. *Biometals* **17**, 235–243
- 31 Gray-Owen, S. D. and Schryvers, A. B. (1996) Bacterial transferrin and lactoferrin receptors. *Trends Microbiol.* **4**, 185–191
- 32 Schryvers, A. B. and Stojiljkovic, I. (1999) Iron acquisition systems in the pathogenic *Neisseria*. *Mol. Microbiol.* **32**, 1117–1123
- 33 Gómez, J. A., Criado, M. T. and Ferreirós, C. M. (1998) Cooperation between the components of the meningococcal transferrin receptor, TbpA and TbpB, in the uptake of transferrin iron by the 37-kDa ferric-binding protein (FbpA). *Res. Microbiol.* **149**, 381–387
- 34 Shouldice, S. R., McRee, D. E., Dougan, D. A., Tari, L. W. and Schryvers, A. B. (2005) Novel anion-independent iron coordination by members of a third class of bacterial periplasmic ferric ion-binding proteins. *J. Biol. Chem.* **280**, 5820–5827
- 35 Shouldice, S. R., Skene, R. J., Dougan, D. R., Snell, G., McRee, D. E., Schryvers, A. B. and Tari, L. W. (2004) Structural basis for iron binding and release by a novel class of periplasmic iron-binding proteins found in Gram-negative pathogens. *J. Bacteriol.* **186**, 3903–3910
- 36 Tom-Yew, S. A., Cui, D. T., Bekker, E. G. and Murphy, M. E. (2005) Anion-independent iron coordination by the *Campylobacter jejuni* ferric binding protein. *J. Biol. Chem.* **280**, 9283–9290
- 37 Gabricevic, M., Anderson, D. S., Mietzner, T. A. and Crumbliss, A. L. (2004) Kinetics and mechanism of iron(III) complexation by ferric binding protein: the role of phosphate. *Biochemistry* **43**, 5811–5819
- 38 Weaver, K. D., Gabricevic, M., Anderson, D. S., Adhikari, P., Mietzner, T. A. and Crumbliss, A. L. (2010) The role of citrate and phosphate anions in the mechanism of iron(III) sequestration by ferric binding protein: kinetic studies of holoprotein formation of wild type and engineered mutants of FbpA. *Biochemistry* **49**, 6021–6032

Received 14 July 2010/19 August 2010; accepted 27 August 2010

Published as BJ Immediate Publication 27 August 2010, doi:10.1042/BJ20101043

SUPPLEMENTARY ONLINE DATA

The role of vicinal tyrosine residues in the function of *Haemophilus influenzae* ferric-binding protein A

Husain K. KHAMBATI*, Trevor F. MORAES†, Jagroop SINGH*, Stephen R. SHOULDICE‡, Rong-hua YU* and Anthony B. SCHRYVERS*¹

*Department of Microbiology and Infectious Diseases, University of Calgary, 3330 Hospital Drive NW, Calgary, Canada, T2N 4N1, †Department of Biochemistry, University of Toronto, 1 Kings College Circle, Toronto, Canada, M5S 1A8, and ‡Institute for Molecular Bioscience, The University of Queensland, 306 Camody Rd, Brisbane, QLD 4072, Australia

SUPPLEMENTARY EXPERIMENTAL

Preparation and cloning of mutant genes

Site-directed mutant genes were prepared from the wild-type *fbpA* gene from *H. influenzae* strain DL63 cloned in a pT7–7 expression vector [1] by the QuikChange™ mutagenesis protocol (Sigma) or by overlapping PCR [1a]. Complementary oligonucleotides were designed to replace the respective tyrosine residue with the indicated amino acid and, through silent mutation, a restriction site that could be used to verify creation of the desired construct. The wild-type and mutant genes were amplified with primers introducing an in-frame BamHI site preceding the region encoding the first amino acid of the mature coding sequence and XbaI after the stop codon. The PCR products were subcloned into an intermediate vector and sequenced. The resulting plasmids were digested with BamHI and XbaI and the *fbpA* genes subcloned into a derivative of the pT7–7 expression vector for recombinant protein production. The modified vector was obtained by first cloning the intact *fbpA* gene amplified from genomic DNA into the EcoRI site of the pT7–7 vector and then performing inverse PCR introducing a BamHI site immediately after the region encoding the leader peptide of FbpA and an XbaI site immediately upstream of the vector HindIII site. The BamHI restriction site engineered at the beginning of the mature coding sequence introduced an N-terminal glycine and serine residue into the wild-type and mutant proteins used in the present study, which was unlikely to have an impact on the properties of these proteins. QuikChange™ mutagenesis was performed on plasmid pSC590 [2] to generate the mutations for evaluating function in the *E. coli* reporter strain.

Protein production and characterization

The expression plasmids encoding the mutant and wild-type *H. influenzae* FbpAs were transformed into strain C43 [3]. The resulting strains were grown on LB (Luria–Bertani) medium and protein production was induced by the addition of 0.5 mM isopropyl β -D-thiogalactopyranoside followed by incubation at 37°C overnight. Relatively pure preparations of protein were obtained from a modified osmotic-shock procedure [4]. Centrifugation ultrafiltration at 4°C was used to exchange the buffer to 10 mM Hepes, pH 8.0, and the resulting samples were applied to a Q-Sepharose anion-exchange column. FbpA was present in the initial flow-through, while contaminants remained bound to the column. A 10-fold molar excess of ferric citrate was added to concentrated samples of the flow-through, after which the buffer was exchanged with 10 mM Hepes, pH 8.0. SDS/PAGE was performed to confirm the purity of the protein preparations

(results not shown), which were subsequently stored at –80°C until they were used for crystallography or functional analyses.

Analysis of iron binding

Absorption spectra were obtained for the iron-loaded protein samples to identify the absorption maxima for the iron–tyrosyl interaction. A citrate-competition assay was performed to determine the affinity constant for iron binding [1]. For this assay, samples were adjusted to 100 μ M FbpA protein in 10 mM Hepes, pH 8.0, with concentrations of sodium citrate (pH 8.0) varying from 0 to 500 mM. After incubation overnight at 4°C, the spectra were recorded with a Bio-Tek Synergy HT 96-well plate reader. The citrate concentration required to remove 50% of iron from FbpA was determined in three experiments and used to calculate the affinity-binding constants as described previously [1].

In vivo β -galactosidase assay

Plasmids derived from pSC590 carrying the wild-type or mutant *fbpA* genes (plus the wild-type *fbpB* and *fbpC* genes) were used to transform *E. coli* strain H1771 [5]. This strain is defective in iron acquisition and has a Fur-regulated β -galactosidase such that enzyme activity reflects intracellular iron concentration. Transformants were screened on MacConkey agar plates supplemented with 40 μ M ferrous sulfate plus antibiotic, providing a preliminary assessment between functional (white colonies) and non-functional (red colonies) iron-transport pathways.

The β -galactosidase was quantitatively measured as described previously [6] to provide an indirect measurement of iron uptake by the FbpABC transporter. Briefly, strains were grown overnight at 37°C in 2 ml of LB broth containing 100 μ M FeSO₄ plus antibiotics. The following day, 20 μ l of culture was transferred to a black/clear flat-bottomed 96-well plate containing 80 μ l of Z-buffer (100 mM sodium phosphate, 10 mM KCl, 1 mM MgSO₄ and 50 mM 2-mercaptoethanol, pH 7.0). Cell density was measured at 600 nm. A 25 μ l aliquot of a 1 mg/ml solution of MUG (4-methylumbelliferyl β -D-glucopyranoside) substrate in DMSO was added to the well and the sample was incubated at room temperature (21°C) for 15 min. The enzymatic reaction was stopped with 30 μ l of 1 M Na₂CO₃. The amount of fluorescence generated by β -galactosidase-dependent MUG hydrolysis was quantified in a microplate fluorimeter ($F_{360/460}$), using samples from cell-free culture medium as a blank. β -Galactosidase

¹ To whom correspondence should be addressed (email schryver@ucalgary.ca)

The four refined crystal structures of FbpA determined in the present study will appear in the PDB under accession codes 3KN7 (Y195A), 3KN8 (Y196A), 3OD7 (wild-type closed) and 3ODB (wild-type open).

Table S1 Crystallization conditions

MME, monomethylether; PEG, poly(ethylene glycol).

Protein	Sample conditions	Crystallization conditions	Crystal colour	Temperature
Closed Fe-loaded FbpA	30 mg/ml in 10 mM Hepes, pH 7.0	18 % PEG 4000, 0.4 M imidazole/malate, pH 6.6 and 0.2 M NaCl	Purple	30 °C
Open Fe-loaded FbpA	80 mg/ml in 10 mM Hepes, pH 7.4	25 % PEG 1000, and 0.1 M Mes pH 6.5	Orange	20 °C
Y195A mutant Fe-loaded FbpA	34 mg/ml in 10 mM Tris/HCl, pH 8.0	34 % PEG 550 MME and 0.1 M Tris/HCl, pH 7.6	Orange	4 °C
Y196A mutant Fe-loaded FbpA	32 mg/ml in 10 mM Tris/HCl, pH 8.0	28 % PEG 550 MME and 0.1 M Tris/HCl, pH 8.5	Orange	20 °C

Table S2 Summary of the X-ray data collection and refinement statistics

(a) Data set

	Closed wild-type	Open wild-type	Y195A mutant	Y196A mutant
PDB code			3KN7	3KN8
Space group	P2 ₁ 2 ₁ 2	P2 ₁ 2 ₁ 2	P2 ₁ 2 ₁ 2	P2 ₁ 2 ₁ 2
Unit cell (<i>a, b, c</i> in Å)	<i>a</i> = 132, <i>b</i> = 52, <i>c</i> = 41	<i>a</i> = 106, <i>b</i> = 77, <i>c</i> = 34	<i>a</i> = 106, <i>b</i> = 76, <i>c</i> = 34	<i>a</i> = 106, <i>b</i> = 76, <i>c</i> = 33

(b) Data collection

	Closed wild-type	Open wild-type	Y195A mutant	Y196A mutant
Resolution (Å)	1.80	1.62	1.70	1.90
Completeness (%)	96.52	95.90	96.70	92.30
<i>I</i> / σ (<i>I</i>)	27.3	40.0	15.2	9.9
<i>R</i> _{sym}	0.039	0.053	0.044	0.049
Redundancy	4.9	13.2	6.5	3.0

(c) Refinement statistics

	Closed wild-type	Open wild-type	Y195A mutant	Y196A mutant
Resolution (Å)	1.80	1.62	1.70	1.90
Completeness for range (%)	96.52	95.90	98.90	91.40
Number of reflections	24756	32432	28694	19046
<i>R</i> -factor	0.23076	0.23273	0.190	0.184
<i>R</i> _{free}	0.26484	0.26624	0.237	0.235
Number of protein atoms	2536	2567	4551	4534
Number of water molecules	164	270	369	247
Number of Fe atoms	1	1	1	1
Mean <i>B</i> -factors (Å ²)	26.946	15.154	13.95	17.56
Bond lengths (Å)	0.007	0.007	0.011	0.009
Bond angles (°)	0.941	0.988	1.200	1.155

activity was calculated by standardizing for time and cell density:

$$\beta\text{-Galactosidase activity} = \frac{F_{360/460}}{t \times D_{600}}$$

The inverse of the activity was calculated in order for values to reflect the levels of iron in the cytoplasm and the values relative to the average obtained with the wild-type protein were expressed as a percentage to best illustrate the relative ability to mediate iron transport.

Crystallography and structure determination

Iron-loaded protein samples removed from -80°C were placed on ice to thaw and were used directly, or after buffer exchange, by centrifugation ultrafiltration. Samples of the Q58L protein [1,7] were included in these studies as they were considered the most likely to crystallize in the closed conformation. Crystals of the wild-type and mutant FbpA proteins were grown by vapour diffusion using the hanging-drop technique with a range

of protein concentrations and incubation temperatures. Initial screens were performed around conditions reported in published studies [8,9], resulting in diffraction-quality crystals for the wild-type protein within 1–2 days (Table S1). Preliminary diffraction analysis of crystals obtained from the wild-type proteins revealed unit cell dimensions (*a* = 132, *b* = 52, *c* = 41) comparable with the published structure when the imidazole/malate buffer was used, but crystals obtained with the Mes buffer yielded unit cell dimensions (*a* = 106, *b* = 77, *c* = 34) comparable with those obtained in previous studies with mutant proteins that were in the open conformation. These results suggested that only crystals from screens with the imidazole/malate buffer were in the closed conformation. Unfortunately, all of the crystals obtained with mutant FbpAs in the imidazole/malate buffer had unit cell dimensions reflecting protein in the open conformation, including Q58L, thus structural determination of these preparations was not pursued. To obtain crystals of the Y195A and Y196A proteins, which were of particular interest for the present study, preparations of protein with added phosphate [4] were also used and screened around conditions that were successful for prior structural determination of mutant proteins. Crystals obtained

under conditions listed in Table S1 provided good diffraction properties and were used for structural determination.

As an alternate approach for obtaining crystals of mutant proteins in the closed conformation, the wild-type crystals from the imidazole/malate buffer were used in microseeding experiments. The rationale for this approach is that crystals of mutant proteins formed from seeding with the wild-type protein in the closed conformation would conform to the existing crystal lattice and result in crystals containing mutant proteins in the closed conformation. Unfortunately, all of the crystals of the mutant proteins screened around these crystallization conditions had unit cell dimensions consistent with protein in the open conformation. The probable explanation is that crystallization could be readily attained under these conditions without microseeding and thus overwhelmed any attempts at crystallization in the closed conformation.

For cryo-crystallography, crystals were dipped into a cryoprotectant solution identical with the reservoir solution with a final concentration of 20% (v/v) ethylene glycol for a short time before being cryo-cooled in liquid nitrogen. Diffraction data revealed that all crystals belong to the orthorhombic space group $P2_12_12$ with the cell parameters outlined in Table S2 and with one subunit in the asymmetric unit. All X-ray data sets were collected from single crystals at 100 K using cryo-mounting procedures. Data collected in-house using a Rigaku 007 Micromax Cu-K α generator (CuK α radiation, $\lambda = 1.542 \text{ \AA}$) or at the Advanced Light Source beamline 8.2.2 and were processed using HKL2000 software. Individual data-processing statistics for the metal-binding mutants are listed in Table S2 as are the PDB codes for the submitted structures.

Structure solution and refinement

Structures of FbpA derivatives were determined by molecular replacement (MolRep CCP4) using the structure of apo *H. influenzae* (PDB accession code 1D9V) as an initial search model. Five percent of the reflections were set aside for calculation of a free *R*-factor. Iterative cycles of manual model building and

refinement were performed using Coot and Refmac5 to complete and correct each model. Water molecules were incorporated into each model using the program ARP/wARP. Electron density for the terminal Lys³⁰⁹ residue within both the 3ODB and 3OD7 structures was uninterpretable and not modelled during refinement. Individual refinement statistics for the metal-binding mutants are displayed in Table S2.

REFERENCES

- 1 Khan, A. G., Shouldice, S. R., Kirby, S. M., Yu, R.-H., Tari, L. W. and Schryvers, A. B. (2007) High affinity binding by the periplasmic iron-binding protein from *Haemophilus influenzae* is required for acquiring iron from transferrin. *Biochem. J.* **404**, 217–225
- 1a Horton, R. M., Cai, Z., Ho, S. N. and Pease, L. R. (1990) Gene splicing by overlap extension: tailor-made genes using the polymerase chain reaction. *Biotechniques* **8**, 528–535
- 2 Adhikari, P., Kirby, S. D., Nowalk, A. J., Veraldi, K. L., Schryvers, A. B. and Mietzner, T. A. (1995) Biochemical characterization of a *Haemophilus influenzae* periplasmic iron transport operon. *J. Biol. Chem.* **42**, 25142–25149
- 3 Miroux, B. and Walker, J. E. (1996) Over-production of proteins in *Escherichia coli*: mutant hosts that allow synthesis of some membrane proteins and globular proteins at high levels. *J. Mol. Biol.* **260**, 289–298
- 4 Shouldice, S. R., Dougan, D. R., Skene, R. J., Tari, L. W., McRee, D. E., Yu, R.-H. and Schryvers, A. B. (2003) High resolution structure of an alternate form of the ferric-ion binding protein from *Haemophilus influenzae*. *J. Biol. Chem.* **278**, 11513–11519
- 5 Hantke, K. (1987) Selection procedure for deregulated iron transport mutants (*fur*) in *Escherichia coli* K 12: *fur* not only affects iron metabolism. *Mol. Gen. Genet.* **210**, 135–139
- 6 Vidal-Aroca, F., Giannattasio, M., Brunelli, E., Vezzoli, A., Plevani, P., Muzi-Falconi, M. and Bertoni, G. (2006) One-step high-throughput assay for quantitative detection of β -galactosidase activity in intact Gram-negative bacteria, yeast, and mammalian cells. *BioTechniques* **40**, 433–440
- 7 Ekins, A., Khan, A. G., Shouldice, S. R. and Schryvers, A. B. (2004) Lactoferrin receptors in Gram-negative bacteria: insights into the iron acquisition process. *Biometals* **17**, 235–243
- 8 Bruns, C. M., Norwalk, A. J., Avrai, A. S., McTigue, M. A., Vaughan, K. A., Mietzner, T. A. and McRee, D. E. (1997) Structure of *Haemophilus influenzae* Fe⁺³-binding protein reveals convergent evolution within a superfamily. *Nat. Struct. Biol.* **4**, 919–924
- 9 Shouldice, S. R., Skene, R. J., Dougan, D. A., McRee, D. E., Tari, L. W. and Schryvers, A. B. (2003) The presence of ferric-hydroxide clusters in mutants of the *Haemophilus influenzae* ferric ion-binding protein A. *Biochemistry* **42**, 11908–11914